MODEL EXPERIMENT AND NUMERICAL SIMULATION OF SURFACE EARTHQUAKE FAULT INDUCED BY LATERAL STRIKE SLIP

Muneo HORI[1], Maciej ANDERS[2] and Hirohide GOTOH[3]

[1]Earthquake Research Institute, University of Tokyo (Yayoi, Bunkyo, Tokyo 113-0032, Japan)
[2]former Ph.D. student, Earthquake Research Institute, University of Tokyo
[3]former ME student, Earthquake Research Institute, University of Tokyo

This paper presents the models experiment and the numerical simulations of a surface earthquake fault which is induced by the lateral strike slip of the bedrock mass. These studies are made to observe and reproduce the evolution of the fault within soft layers. In the model experiments, the successive bifurcation processes are observed, and they lead to large variability of the faults. The numerical simulation uses a stochastic finite element method which estimates the variability of the fault behavior. Such a stochastic analysis method is a promising tool, since it is able to account for the bifurcation processes and the variability.

Key Words : *surface earthquake fault, active fault, bifurcation, strain localization*

1. INTRODUCTION

In Turkey and Taiwan earthquakes of 1999, surface earthquake faults were formed in urban areas, causing severe damages to near-by social infrastructures such as highways and dams[1]. While a threat of such surface faults has not been fully ignored, these events arose to cautions to a possibility of the surface fault formation and the resulting catastrophic disaster. Japan has numerous active faults which lie throughout the islands[2]. For the safety of civil structures, therefore, it will be required to predict the possibility of the surface fault formation caused by a large earthquake that moves an active fault, as well as the location and the displacement of the fault in a case when the surface fault is formed on the ground surface.

While strong motion hits near-by cities when a large earthquake takes place, surface faults do not always appear on ground surfaces. In Japanese earthquake engineering, therefore, little attention has been paid to damages caused by the possible surface earthquake formation, except for a few cases such as the construction of nuclear power plants and large dams. On the other hand, geological researches of the active faults have been extensively made in Japan since 1960's, and two active fault maps that cover the Japanese Islands were made[2]. Geophysical researches clarify the rate

of the crustal deformation due to the plate tectonics, and, for a given active fault, the maximum displacement of a possible surface fault can be estimated by using the crustal deformation. These data can be used to predict the location and the displacement for a possible earthquake. The accuracy, however, may not be enough. In particular, the value of the displacement may be considerably overestimated, since the dispersion of fault displacements within surface alluvia or soft surface deposits on the bedrock mass is ignored.

For the prediction of the surface earthquake faults, limited researches have been made, since the prediction was less needed as well as the formation processes are complicated. Among them, we point out Bray and his colleagues[3],[4], who developed numerical computation methods for the fault behavior analysis (see also the related researches[6],[5]), and Tani and Ueta[7] for the model experiments of the fault formation (see also similar model experiments[8]).

The variability the surface earthquake fault should be taken into consideration, in predicting the possible fault formation. On the length scale of $10^{1\sim2}$[m], a fault consists of several segments which may curve or kink. The displacement of the segments varies from place to place and even vanishes at some regions. Such high variability of the surface fault segments leads to the unpredictability of the fault behavior. This is because the surface layer deposit has complicated struc-

tures and does not allow the formation of a fault of simple configuration. The movement of the bedrock might be complicated as well. For the mechanical point of view, the fact that the fault formation involves a bifurcation phenomenon is not overlooked; for instance, the lateral strike slip of the bedrock usually causes a set of echelon of faults on the ground surface, instead of one fault line that is extended from the bedrock fault.

In order to rationally predict the behavior of a possible surface earthquake fault, we have to clarify the mechanisms of the fault formation that leads to the high variability. We also need to develop a reliable analysis method which can accounts for the uncertainty of the structures and properties of surface layer deposit. To this end, we[11),12),13),20)] carried out model experiments and numerical simulations for the surface fault formation that was induced by the lateral strike slip of the bedrock mass. The model experiments[13),20)] use transparent gelatin samples such that the whole processes of the fault formation can be observed. The numerical simulation[16),18),19),20)] is aimed at developing an analysis method for predicting the surface fault behavior. To estimate the variability, the method calculates the mean and variation of the fault behavior such as displacement and strain, by using a stochastic model for uncertain surface deposits.

In this paper, we summarize recent results of our studies on the surface fault formation. Sections 2 and 3 present the model experiments and the numerical simulation, respectively. Some future works which we think are needed for the development of a reliable analysis method are discussed in Section 4.

2. MODEL EXPERIMENTS

The objective of the model experiments[13),20)] is to observe the whole processes of the surface fault formation. Special attention is paid to the mechanism that leads to the high variability of the fault behavior. A flat disk-shaped transparent gelatin specimen is used as a model of a surface deposit. The specimen is made by poring hot gelatin solution to the experimental apparatus, and the solution is solidified to form a homogeneous test sample. The thickness of the specimen is changed from 1[cm] to 3[cm]. The specimen is attached on the flat iron disk, and the torsional shearing is applied to its bottom, by gradually rotating the inner circular part of the disk with the outer annular region of the disk being fixed. In this manner, uniform lateral strike slip is caused on the bottom of the specimen; see **Fig. 1**. For a higher repeatability of

a) torsional shearing

b) experiment apparatus
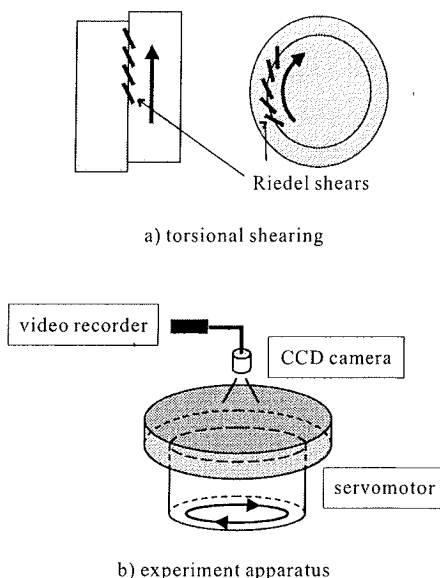
Fig. 1 Schematic view of model experiment.

the experiment, samples are made carefully by controlling the temperatures and using gelatin solution of high concentration. Also, the torsional shearing is applied by controlling the rotation speed with the servo-system. The applied torque is measured to examine the relation between the amount of the rotation and the torque. For all experiments, the difference in the rotation for a given torque is less than 10%.

It is observed that cracks are initiated along the boundary of the circular part and the annular region, and gradually grow upwards as the slip increases. The cracks finally reach the top, and produce Riedel shears, i.e., a periodic array of more or less parallel but oblique cracks. The length, orientation and number of the cracks that appear on the top surfaces are measured. A CCD camera is used to observe the initiation, growth and appearance processes. Three sets of horizontal grid patterns are put into the specimen, to measure the horizontal deformation of the bottom, middle and top layers. The image analysis is applied to compute displacement and strain from the movement of the grid. These data of the deformation are used to estimate the constitutive relations of gelatin sample by applying the *stress inversion* such that the experimental data will be reproduced in a suitable numerical simulation; see Appendix A for the stress inversion.

The key observations of the model experiments are summarized as follows:
1) small micro-cracks of length 1[mm] are periodically

a) successive bifurcation of crack growth

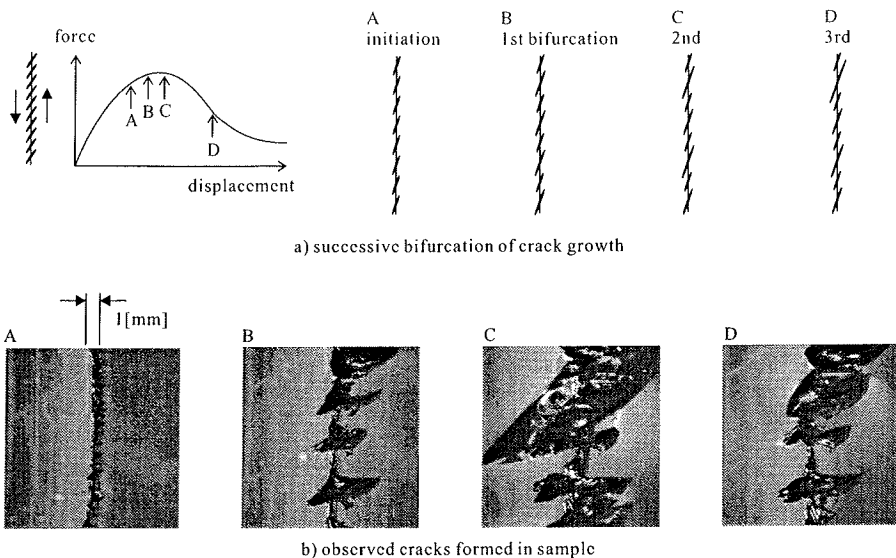b) observed cracks formed in sample

Fig. 2 Summary of model experiment observation.

initiated along the boundary, with the distance between adjacent cracks being 1[mm] (the initiation process);

2) all cracks grow equally as the bottom slip increases, until every second crack keeps growing while the growth of the others is stopped (the first bifurcation);

3) similar bifurcation processes are repeated, and every fourth or eighth crack keeps growing (the second or third bifurcation);

and 4) growing cracks appear on the top, forming an echelon pattern, being slightly oblique with respect to the slip direction.

Such successive bifurcation processes lead to the large variability of the crack behavior. **Figure 2** presents the summary of these processes, together with photos taken by the CCD camera.

While the observed processes are more or less similar to all experiments, the configuration of the cracks that finally appear on the surface differs from specimen to specimen. Furthermore, some specimens have large and small cracks while most of specimens have more or less similar cracks. This is mainly because the bifurcation is involved in the crack evolution. **Table 1** summarizes the conditions of 31 specimens used and the configuration of cracks that finally appear on the top surfaces; h, v, T and ρ are the thickness, loading speed, temperature and density of the sample, and L, θ and N are the average length, orientation and number of the surface crack; and a symbol " ? " stands for

that the quantity is not accurately measured. Some relations between the thickness and the crack configuration are seen; smaller N and L for lager h. However, the variability of the crack configuration is large. For specimens of 1[cm] thickness, N ranges from 13 to 39 and L ranges from 2[cm] to 16[cm]; see **Fig. 3**.

By analyzing the images of the grid patterns that is put in the specimen, we calculate strain in order to study the deformation inside of the specimen. The small deformation is assumed in the calculation even though the value of strain goes over 100% and differentiation is replaced by finite difference. As a typical example, the distribution of the maximum shear strain at the middle plane of the specimen is presented in **Fig. 4**. It is seen that large shear strain is caused around the crack that passes the middle plane. While the material is different, we can expect that large shear strain will be caused within the surface deposit, such that the growth of the faults is resisted by dispersing the strain energy to produce large deformation around the growing faults. Thus, more strain energy will be consumed as the failure of the surface deposit materials requires more energy or as the thickness of the surface layers increases.

While the size and the material are different, we can expect that actual surface earthquake faults will be formed through essentially the same mechanism as observed in the model experiments and that the successive bifurcation processes take place; *flower structures* of the actual fault correspond to a set of faults

Table 1 Summary of crack configuration observed in model experiments.

id	h [cm]	v [cm/sec]	T °C	ρ [cm³/g]	L [cm]	θ [deg]	N
1	1.00	0.3094	11.0	?	?	?	38
2	0.95	0.0518	17.0	?	5.3	33.69	13
3	0.98	0.2473	15.0	?	4.6	22.62	35
4	0.89	0.0417	?	?	4.7	35.54	34
5	0.85	0.0559	?	0.899	?	?	33
6	0.90	0.4211	18.0	0.910	9.8	29.25	23
7	0.91	0.4660	18.0	0.910	10.3	26.57	25
8	0.89	0.7413	18.0	0.899	11.8	24.70	28
9	1.10	0.0497	19.0	0.922	6.2	29.54	34
10	1.00	0.0315	12.5	0.999	11.6	30.96	21
11	1.10	0.0233	13.0	?	9.7	40.60	24
12	1.10	0.0306	12.0	0.082	6.8	45.00	29
13	0.90	0.0351	13.0	0.900	7.7	48.37	32
14	1.00	0.0715	12.5	0.990	2.0	41.01	26
15	0.80	0.0410	14.5	0.988	7.8	32.01	29
16	0.93	0.0719	13.5	0.981	5.7	37.19	31
17	1.90	0.0767	19.2	0.900	13.0	9.090	15
18	1.80	0.0669	18.0	0.945	12.8	12.99	19
19	1.60	0.0342	19.5	0.928	9.3	25.56	20
20	2.00	0.0773	16.9	?	15.3	41.12	13
21	2.00	0.0187	16.1	0.921	10.5	12.76	17
22	2.00	0.0631	13.0	0.985	10.5	35.42	17
23	1.90	0.0453	14.0	0.987	9.0	32.01	18
24	1.85	0.0312	14.5	?	10.3	45.00	22
25	2.20	?	17.0	?	14.0	31.40	9
26	2.40	0.0263	15.0	?	10.0	48.09	15
27	1.80	0.0505	11.0	0.988	10.0	45.00	17
28	1.80	0.0300	13.5	1.005	7.3	43.36	19
29	2.10	0.0479	12.0	0.983	11.5	49.40	25
30	1.70	0.0449	10.0	0.984	10.0	50.19	19
31	3.00	?	20.0	0.935	13.0	8.130	13
32	3.00	?	19.0	?	16.0	10.01	8

that are forced to stop at various depth during the bifurcation processes. For the lateral strike slip of the bedrock mass, more energy is consumed by creating echelon faults, compared with just by extending the slip to one plane of an active fault. In the theoretical analysis[11],[17],[21], we show that for a homogeneous body subjected to uniform loading, the bifurcation takes place when the body is fractured and periodic damages are created within the body. We also show that the alternative evolution is most likely to occur when the uniform growth of periodic damages within the homogeneous body is bifurcated. (This is consistent with the results of the model experiments, since the number of the surface crack tend to be half as the specimen thickness; see **Fig. 3.**) These theoretical analyses support our hypothesis that the successive bifurcation processes will happen during the growth of the surface earthquake faults within the surface deposit layers. For the mechanical point of view, therefore, it is expected that the surface faults are

not formed unless the bedrock mass produces work enough to cause complicated failure throughout the surface layers, and that, even if the faults appear on the ground surface, the displacement is smaller than the slip of the bedrock mass.

3. NUMERICAL SIMULATIONS

It is certainly true that various phenomena must be analyzed to predict the surface fault formation. However, such analysis may not be meaningful owing to the uncertainty of the underground structures. The surface layers on the bedrock mass are most reliably identified, and the effects of the deposits on the failure energy dissipation can be significant. Therefore, we seek to analyze the rupture processes in the surface layers, provided that the configuration and the maximum displacement of the fault in the bedrock mass are known. In the analysis, surface layers are modeled as a body consisting of heterogeneous elasto-
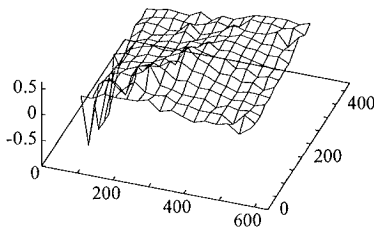
number of Riedel shear
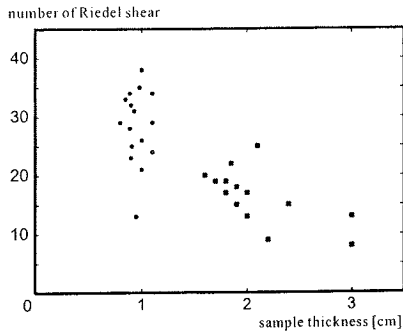
a) relation between thickness and length

length of Riedel shear[cm]
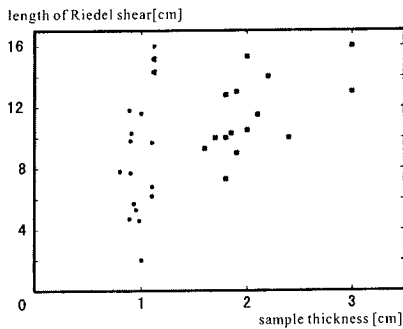
b) relation between thickness and number

Fig. 3 Change in number and length of crack with respect to sample thickness.

Fig. 4 Distribution of maximum shear strain in middle of sample.

plastic materials and faults as zones of localized plastic strain[16),18)] rather than cracks[12),14)]. It should be emphasized that the surface layer model is *stochastic* in a sense that the mean and the standard deviation are given to the material properties and the configuration of each layer; the standard deviation, which accounts for the uncertainty of the layers, takes a larger value in a case the uncertainty of the surface layers is larger due to the limitation of the in-sit measurements. The analysis, therefore, is stochastic such that the variability is computed for the responses of the

stochastic model. It also takes into consideration the bifurcation processes; the pattern of the fault evolution changes drastically due to the bifurcation.

In order to analyze a stochastic elasto-plastic body, we are developing[19),20)] a new *stochastic finite element method* (SFEM) that computes the probabilistic characteristics, such as the mean, the variance, the correlation and the probability density function (PDF), for displacement, strain and stress fields. Unlike ordinary SFEM which is based on the perturbation expansion to small stochastic variability, the developed SFEM is capable to analyze the probabilistic characteristics efficiently even for large stochastic variability. This is because it makes use of the Karhunen-Loeve (KL) and the polynomial chaos (PC) expansions to the stochastic model properties and the corresponding stochastic responses, respectively; see Appendix B. The advantage of these expansions in solving linear stochastic problem is known and the developed SFEM extends it to the non-linear problems. It is shown that if a few terms are taken in these expansions, complicated probabilistic characteristics can be accurately computed. Furthermore, we should point out that the developed SFEM automatically chooses the mode that is most likely to occur when the bifurcation takes place. This is mainly because stochastic modeling of the elasto-plastic body results in smoothing the constitutive relations that have discontinuous changes in the instantaneous moduli at the transit from the plastic loading to the elastic unloading. The stochastic moduli change continuously if some variability of the constitutive relations is accounted for and the transit to the elastic unloading gradually takes place (i.e., the probability of the unloading increases from 0% to 100% as the external load increases). Thus, once the bifurcation takes place, the iteration scheme of the computation can find the most (numerically) unstable solution much easier than the original non-linear equations of the elasto-plastic body that have discontinuous change in the instantaneous moduli.

In order to demonstrate the usefulness of the developed SFEM, we show in **Fig. 5** the comparison with the Monte-Carlo simulation (MCS), for a two-dimensional problem of a stochastic elasto-plastic material sample subjected to deterministic concentration loading. The PDF of a displacement component at which the load is applied is shown in the figure; a) and b) are for the vertical and horizontal components, respectively. It is shown that the SFEM can estimate two different PDF's, a log-normal distribution for the vertical displacement and a normal distribution for the
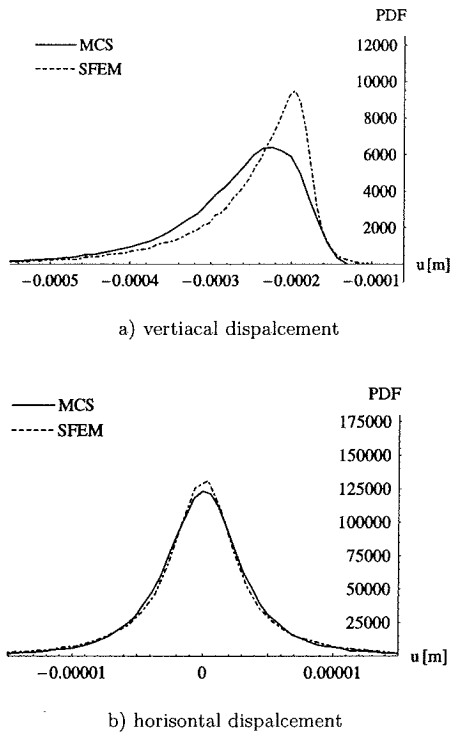
a) vertiacal dispalcement

b) horisontal dispalcement

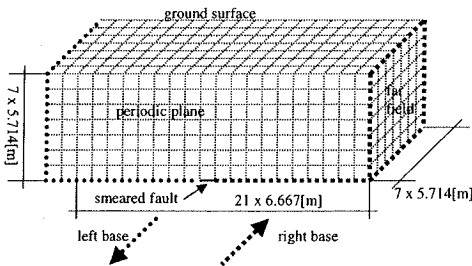**Fig. 5** Comparison of SFEM with Monte-Carlo simulation.

Fig. 6 Stochastic model of numerical simulation.

horizontal component, and that the agreement with the MCS is satisfactory. The number of the terms used in the KL and PC expansions is 4 and 2, respectively, and hence the numerical complexity is increased just 10 times even though all the terms in the expansions are numerically computed.

In order to examine the applicability of the SFEM to the surface fault problem, we consider an idealized case of the rupture process in a stochastic model. The problem setting is as follows: 1) small defor-

mation and quasi-static state are assumed; 2) the dimension of the model is $140\times40\times40$[m]; and 3) the model consists of a stochastically homogeneous material. The elasticity of the material is isotropic and linear; Young's modulus changes stochastically with mean 200[GPa] and the covariance function $Cov(x_1, x_2, x_3) = 0.2\exp((|x_1|+|x_2|+|x_3|))$, but Poisson's ratio is fixed as $\nu = 1/6$. The plasticity of the material is given by a yield function of the associated Drucker-Coulomb type; the compressive and tensile yield stresses are $f_c = 20$[MPa] and $f_t = 2$[MPa]; and the fracture energy release rate of $G_f = 0.06$[N/mm] is used to remove the mesh-dependency of the numerical computation. The prescribed boundary conditions are as follows: 1) traction free conditions on the top surface; 2) periodic displacement and traction on the sides normal to the slip direction; and 3) horizontal rigid body motions of the same amount but the opposite direction are given to right and left parts of the bottom face and the right and left side faces, respectively. The rigid body motion corresponds to the lateral slip of the bedrock mass. **Figure 6** presents a schematic view of this stochastic model

First, we present in **Fig. 7** the evolution of PDF for the maximum shear strain accumulated at the center of the model where the localized shear strain passes; a), b) and c) are for the bedrock slip of 0.015, 0.045 and 0.065[m], respectively. We also carry out the MCS, generating 10,000 bodies according to the given stochastic properties and analyzing the rupture processes of all the bodies. The PDF of the MCS is plotted for the comparison. It is seen in **Figs. 7**a) and c) that the shape of the PDF given by the SFEM is similar to that of the MCS. The large variability of the maximum shear strain is accurately estimated by the SFEM. However, there are three peaks for the PDF of the MCS in **Fig. 7**b), with each peak corresponding to one bifurcated solution. The PDF of the SFEM has one peak, although the location of the peak is close to that of the largest peak of the MCS. The SFEM cannot compute all bifurcated solutions, since the expansion of the SFEM is taken only around the most unstable solution (or the most realizable failure mode) and automatically omits other bifurcated solutions; indeed, the PC expansion used in the SFEM expands probabilistic variables around the mean. This is the limitation of the SFEM. In the present problem, however, bifurcated solutions computed by the MCS eventually merge to one solution, as the PDF has one peak at the bedrock slip of 0.065[m]. It seems that the SFEM reaches the one solution; see that all bifurcated solutions computed by the MCS merge to it.
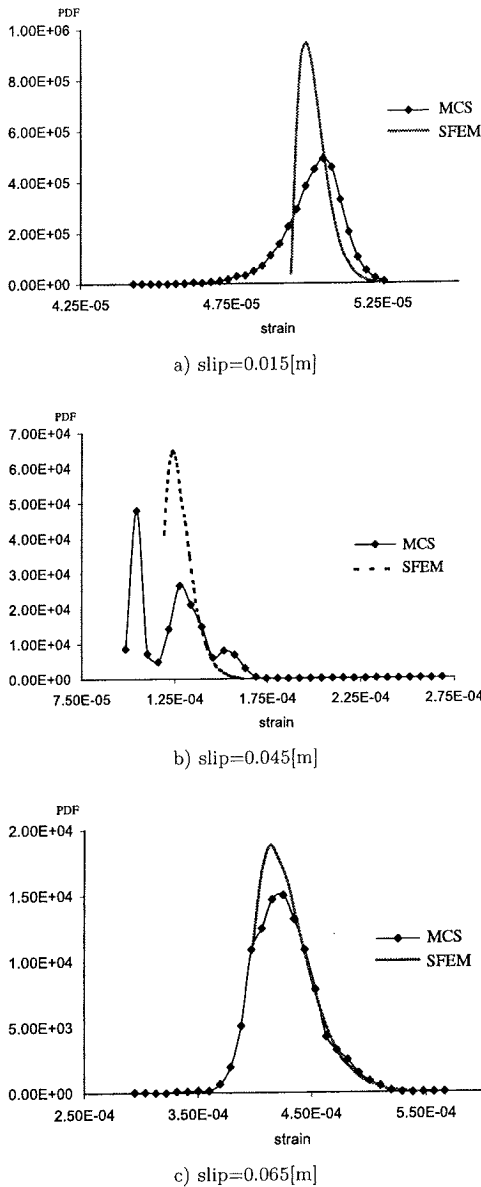
PDF

1.00E+06

8.00E+05

6.00E+05

4.00E+05

2.00E+05

0.00E+00

4.25E-05   4.75E-05   5.25E-05

strain

— MCS
······ SFEM

a) slip=0.015[m]

PDF

7.00E+04

6.00E+04

5.00E+04

4.00E+04

3.00E+04

2.00E+04

1.00E+04

0.00E+00

7.50E-05   1.25E-04   1.75E-04   2.25E-04   2.75E-04

strain

— MCS
- - - SFEM

b) slip=0.045[m]

PDF

2.00E+04

1.50E+04

1.00E+04

5.00E+03

0.00E+00

2.50E-04   3.50E-04   4.50E-04   5.50E-04

strain

— MCS
—— SFEM

c) slip=0.065[m]

Fig. 7 Evolution of PDF of maximum shear strain.

(The rupture processes might be regarded as *chaotic*, since there are many possibilities, due to small difference in the initial configuration, at the initial stage, but these possibilities tend to merge one possibility at the final stages.)

Next, we plot in **Fig. 8** the distribution of the mean and the variance for the maximum shear strain on eight horizontal layers; the layers are equally spaced from the bottom surface to the top surface. Like **Fig.**

7. the distribution at the three bedrock slips. 0.015. 0.045 and 0.065[m]. is plotted from **Fig. 8**a) to **Fig. 8**c). respectively. The evolution of the fault is clearly seen as the localized shear strain goes upwards due to the increase of the bedrock slip. In particular, the distribution of the mean shows that while the maximum shear strain is almost uniform and parallel to the bedrock slip at the bottom surface, it tends to twist just above the bottom surface and eventually forms an echelon pattern at the top surface. The distribution of the variance shows that the variability is large as the value reaches 0.2% at the top surface. It is shown that the segment of the failure is produced as the mean is localized to a narrow band, and that there is a zone around the segment where the variance takes much larger values than the surrounding domains. This zone is probably a place where the surface fault is most likely to be formed. The value of the displacement, if the fault is formed, varies in a wide range.

Although the successive bifurcation processes are not reproduced, the present SFEM can simulate echelon surface faults caused by the simple lateral strike of the bedrock mass; see **Fig. 9** for the mean deformation of the surface. It is certainly true that the computed echelon fault is different from those observed in the reality, as echelon fault is separated at the center. However, the prediction of the variability and the reproduction of the bifurcation are not trivial. In order to demonstrate an application of the SFEM to predict the fault behavior, we compute the mean and the standard deviation (SD) of the displacement caused by the surface fault. **Figure 10** plots the mean and the SD with respect to the bedrock slip; a) and b) are the horizontal and vertical components, respectively, and the mean and the SD are standardized as the ratio to the representative value. As is seen, the fault is dispersed within the soft deposit until the bedrock slip attains a certain value. Once the fault is formed, the displacement increases rapidly. The displacement of the fully formed fault increases almost linearly; due to the elastic resistance that is assumed in the present simulation, the slope of the surface displacement with respect to the bedrock slip is less than 1. The SD of the displacement increases linearly as well, suggesting that the fault behavior can have larger variability after the full formation. Regarding to the bedrock slip, we can observe that there are two critical values, the one at which the surface fault is initiated and the other after which the surface layers are moved as if they are a rigid body fixed to the bedrock. The estimate of these critical values is of primary importance,
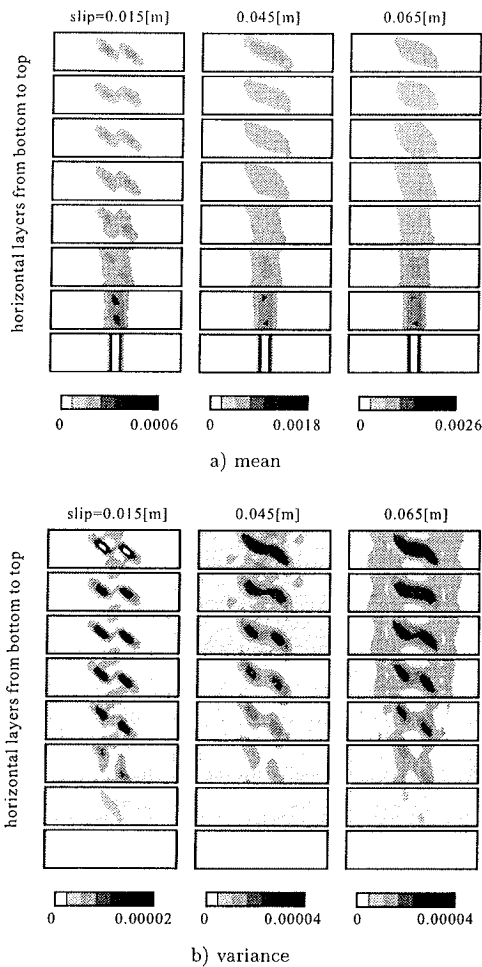
slip=0.015[m]   0.045[m]   0.065[m]

horizontal layers from bottom to top

0   0.0006   0   0.0018   0   0.0026

a) mean

slip=0.015[m]   0.045[m]   0.065[m]

horizontal layers from bottom to top

0   0.00002   0   0.00004   0   0.00004

b) variance

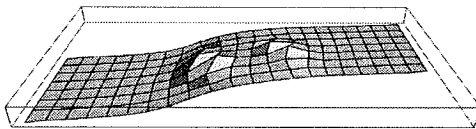**Fig. 8** Distribution of mean and variance of maximum shear strain.

Fig. 9 Surface deformation computed from mean behavior.

since the maximum movement of the source fault can be calculated from the plate movement. It should be noted that these critical values depend on the thickness as well as the material properties of the surface deposits.
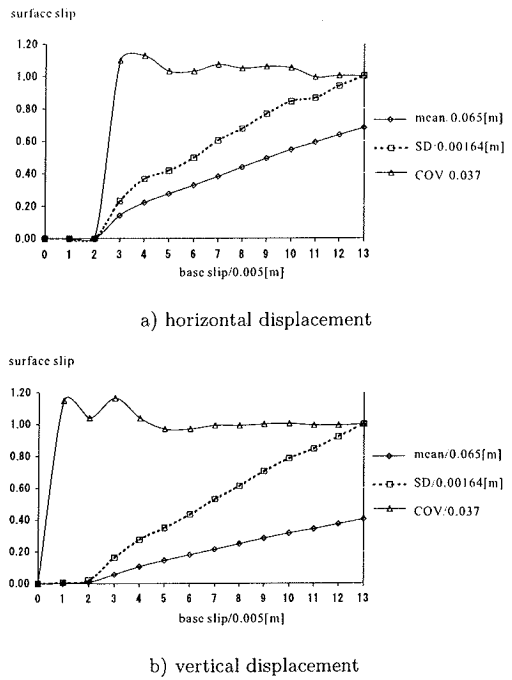

surface slip

— mean. 0.065[m]
··□·· SD·0.00164[m]
—△— COV 0.037

base slip/0.005[m]

a) horizontal displacement

surface slip

— mean/0.065[m]
··□·· SD/0.00164[m]
—△— COV/0.037

base slip/0.005[m]

b) vertical displacement

Fig. 10 Change in mean and SD of surface displacement.

4. CONCLUDING REMARKS

The key results presented in this paper are summarized, as follows:

1. in the model experiment, the successive bifurcation processes are observed, which leads to large variability of the fault formation.
2. the SFEM used in the numerical simulation can solve an example stochastic problem, and the solution agrees with the MCS.

We should point out that, at this moment, we do not succeed to reproduce the experimental results using the developed SFEM; the material properties of gelatin is too complicated to be modeled. However, it is observed that the SFEM can pick up the most unstable solution during the successive bifurcation processes, which will help us reproduce the formation of actual surface faults.

As shown in the preceding section, the SFEM is a promising tool as a candidate of an analysis method for predicting the behavior of a possible surface earthquake fault. Since observed surface faults show high variability, the estimate of the variability of the fault behavior is of essential importance for the analysis method. While the SFEM chases only the most unstable solution among bifurcated solutions, the solution corresponds to the most realizable failure mode. Thus,

considering the computational complexity of the MCS, we can evaluate the SFEM as a reasonable choice. It is expected that the SFEM analysis of the idealized problem leads to a *safe* estimate for the surface displacement, even though the estimate is definitely smaller than the bedrock slip due to the failure dissipation within the surface layers. The estimate of the variability of the fault behavior should be examined by comparing data observed for actual surface earthquake faults. While we think that the bifurcation plays a key role, the analysis method needs to rationally account for other factors which influence the surface fault formation; for instance, the dynamic effects during the formation processes, sliding conditions between fault faces, and more realistic estimates of surface deposit properties should be examined and needed to be installed for the method.

APPENDIX A STRESS INVERSION

The stress inversion method[20] developed by our group is aimed at identifying local constitutive relations of a material sample. The key point of the method is that it can predict the distribution of three stress components for a sample in plane stress or strain state, by measuring the strain distribution on the surface and the traction along the boundary. The basic principle of the method is simple, as it derives boundary value problems for the three stress components from the two equations of equilibrium that the components must satisfy and one known relation between stress and strain.

Our group estimated the local constitutive relations around the crack for gelatin samples applying the stress inversion method. The strain measured by the image analysis and the torque used for the torsional shearing are used for the inversion. A three-dimensional numerical simulation is carried out by using the predicted constitutive relations, in order to reproduce the experimental data. The formation of echelon cracks is reproduced, even though the configuration is different from the observed ones. It should be noted that, in principle, the stress inversion is applicable to the actual surface fault and its constitutive relations are estimated, if the displacement field around the fault is measured by, say, applying the global positioning system or the synthesized aperture radar.

APPENDIX B SFEM

The key feature of the present SFEM[19] is the two expansions that are applied to the variables varying spatially as well as stochastically. The KL expansion is applied to a parameter of a material parameter whose covariance function is given: denoting by x and ω a spatial coordinate and a stochastic event, we can expand the parameter, say, $\alpha = \alpha(x, \omega)$, as

$$\alpha(x, \omega) - \overline{\alpha} = \sum_{m=1}^{\infty} \xi_m(\omega) \sqrt{\lambda_m} \phi_m(x)$$

where $\overline{\alpha}$ is the mean, λ_m and ϕ_m are an eigen-value and an eigen-function of the covariance function, and ξ_m is computed from $\int \alpha \phi_m dx$. The PC expansion uses ξ_m to from a complete orthonormal base in the stochastic space. When ξ_m is discretized as a vector $[\xi]$, the PC expansion provides the base as

$$\Gamma_p([\xi]) = (-1)^p \exp\left(\frac{1}{2}[\xi]^T[\xi]\right)$$
$$\frac{\partial^p}{\partial \xi_{m_1} \cdots \partial \xi_{m_p}} \exp\left(-\frac{1}{2}[\xi]^T[\xi]\right)$$

This Γ_p is explicitly computed, and hence it can be implemented in numerical computation of the finite element method.

It should be emphasized that these stochastic expansions are applied to the incremental behavior that is obtained by linearizing the non-linear equations. In the present SFEM, this linearization is approximately made around the mean of the incremental behavior; the approximation uses a fictitious but deterministic bounding media which are constructed to make optimistic and pessimistic estimates of the mean behaviors. This approximation reduces huge numerical complexity that is inherent to the SFEM, since it expands the stochastic variables to a couple of terms. The algorithm of the SFEM using this approximation is presented in **Fig. 11**.

REFERENCES

1) *Proceedings of Seismic Fault-induced failures* ? Possible remedies for damage to urban facilities ? (ed. By K. Konagai), JSPS Research Project 2000, 2001.
2) Research Group for Active Faults: *Active Faults in Japan: Sheet maps and Inventories* (2nd edition), Univ. Tokyo Press, Tokyo, 1991, (in Japanese).
3) Bray, J.D., Seed, R.B. and Seed, H.B.: Earthquake fault rupture propagation through soil, *J. Geotech. Eng.*, ASCE, Vol. 120, No. 3, pp. 543-561, 1994.
4) Ke, T-C. and Bray, J.D.: Modeling of particulate media using discontinuous deformation analysis, *J. Eng. Mech.*, ASCE, Vol. 121, No. 11, pp. 1234-1243, 1995.
5) Roth, W.H., Kalis, G., Papastamatiou, O. and Cundall, P.A.: Numerical modeling of fault propagation in soils, in *Proc. 4th Int. Conf. on Num. Meth. Geomech.*, pp. 487-494, 1982.
6) Cole, D.A. and Lade, P.V.: Influence zones in alluvium over dip-slip fault, *J. Geotech. Eng.*, ASCE, Vol. 110, No. 5, pp. 599-615, 1984.
7) Tani, K. and Ueta, K.: Shape and location of discontinuity in sand induced by fault displacement in bed rock, in *Proc. 26 Japan National Conf. on Geotech. Eng.*, JSGE, pp. 1185-1188, 1991 (in Japanese).
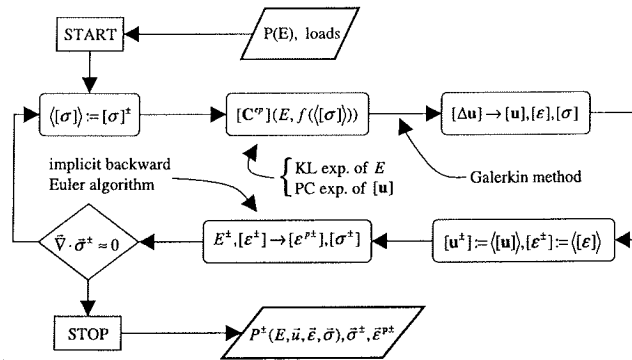
Fig. 11 Algorithm of SFEM.

8) Taniyama, T. and Watanabe, H.: Deformation of sandy deposits by reverse faulting, *J. Struct. Mech. Earthquake Eng.*, JSCE, **591**/I-43, pp. 313-325, 1998.

9) Ohuchi, M., Abe, S., Kusakabe, H. and Hagiwara, T.: Development of shear band and particle crushing observed in in-situ loading tests on a sedimented sand, JSCE, **487**/III-26, pp. 207-216, 1994.

10) Takada, S., Nemat, H. and K. Fukuda: Prpopose of simplified design method for buried pipes crossing earthquake fault, *J. Struct. Mech. Earthquake Eng.*, JSCE, **668**/I-54, pp. 187-194, 2001.

11) Oguni, K., Hori, M. and Ikeda, K.: Analysis on evolution pattern of periodically distributed defects, *International Journal of Solids and Structures*, Vol. 34, No. 25, pp. 3259-3772, 1997.

12) Hori, M. and Vaikuntan, N.: Rigorous formulation of crack path in two-dimensional elastic body, *Mechanics of Materials*, Vol. 26, pp. 1-14, 1997.

13) Hori, M., Oguni, K. and Gotoh, H.: Observation and analysis of initiation process of Riedel shear, *Deformation and Progressive Failure in Geomechanics*, IS Nagoya '97, pp. 509-515, 1997.

14) Hori, M. and Vaikunthan, N.: Analysis of smooth crack growth in brittle materials, *Mechanics of Materials*, Vol. 28, pp. 33-52, 1998.

15) Hori, M. and Vaikunthan, N.: Analysis of the initiation of periodically distributed defects, *Int. J. Plasticity*, Vol. 14, No. 8, 673-688, 1998.

16) Hori, M. and Munashinghe, H.S.: Optimistic/pessimistic behaviors of heterogeneous body with statistically varying material properties, *35th Annual Technical Meeting, Society of Engineering Science, Advanced Modeling in Geomechanics and Minerals Processing*, pp. 69-70, 1998.

17) Hori, M. and Oguni, K.: Bifurcation and stability analyses of initiation and evolution of periodic defects, *Localization and Bifurcation Theory for Soils and Rocks* (ed. by T. Adachi, F. Oka, and A. Yashima), Balkema, Rotterdam, pp. 127-136, 1999.

18) Hori, M. and Munashinghe, H.S.: Generalized Hashin-Shtrikman variational principle for boundary-value problem of linear and non-linear heterogeneous body, *Mechanics of Materials*, Vol. 31, pp. 471-486, 1999.

19) Anders, M. and Hori, M.: Stochastic finite element method for elasto-plastic body, *Int. J. Numer. Meth. Engng.*, Vol. 46, pp. 1897-1916, 1999.

20) Hori, M., Andres. M. and Mizutani, T.: Analysis of periodic shear band formation: experiments and numerical simulation, International Workshop on Bifurcation and Localization, Perth, Australia, November 24-31, 1999.

21) Hori, M. and Oguni, K.: Bifurcating initiation and evolution of periodic micro-defects, *Materials Science and Engineering*, A285, 122-129, 2000.